OBTAINING GRAPHITE OXIDE FROM MECHANICAL GRAPHITE GRINDING

Alex Gomes Pereira

Geotechnical Research Group

Federal University of Amazonas, Brazil

Regina Célia Espinosa Modolo

Professor and Researcher

University of Vale do Rio dos Sinos, Brazil

Benício de Morais Lacerda

Professor and Researcher

Porto Velho School of Education and Culture, Brazil

Jayne Carlos Piovesan

Professor and Researcher

São Lucas University Center, Brazil.

Raduan Krause Lopes

Professor

the Federal University of Rondônia foundation

Abstract

This work sought to obtain graphite oxide from the application of the high-energy ball mill (HEBM). The grinding process occurred by inserting 4 g of the sample of a commercial graphite in the HEBM for the times of 30min, 1 hour and 4 hours. Scanning electron microscopy (SEM) analysis was used for the samples morphological characterization. The analysis of X-ray diffractometry (XRD) allowed to measure the interplanar distances obtained from the comminution of the sample, in addition to evaluating the structural difference between the post-ground samples obtained by the mechanical amorphization process. The results indicated that the increase in the grinding time disturbed the structural order of the graphite and increased the interplanar distance of the post-ground samples in comparison to the precursor graphite.
Keywords: graphite oxide, high energy ball mill, morphological characterization, interplanar distance.

1. Introduction

Carbon is one of the most important chemical elements, as it is indispensable for the existence of life and for exhibiting applications in different areas of knowledge. Carbonaceous materials are those mainly composed of the carbon element, with levels of 99% or more, which can be found in nature or synthetic (MANTEL, 1968; SAVAGE, 1993; MARSH, 1998; CGEE, 2010).

CGEE (2010) explains that carbonaceous materials can be developed from several organic raw materials in solid, liquid or gaseous states. Depending on their formation conditions (natural or processed), carbonaceous materials can be found in several ways. Natural carbonaceous materials have several allotropic forms such as: amorphous carbon (carbon black, common coal, coke, glassy carbon, etc.), crystalline in the form of natural graphite (hexagonal crystalline structure) or diamond (cubic crystalline structure), fullerenes , graphene and carbon nanotube (ZARBIN & OLIVEIRA, 2013). Figure 1 exemplifies some of these configurations.

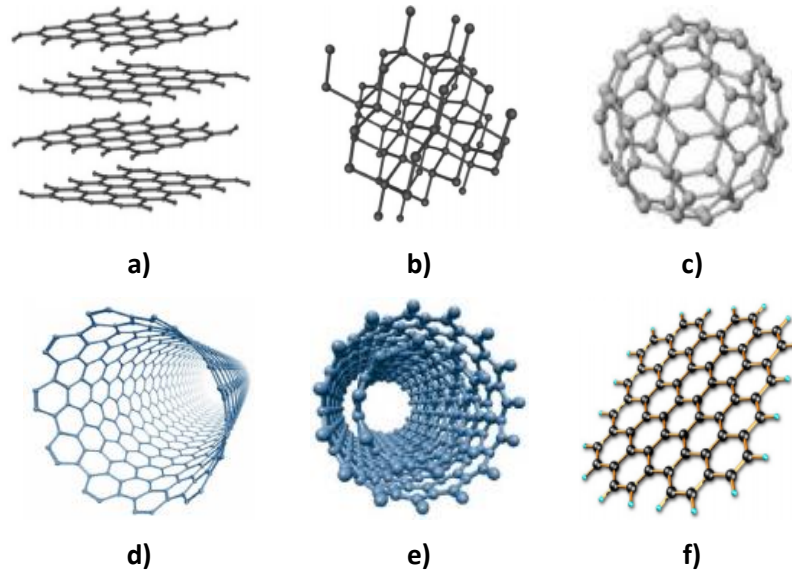**a)**　　　**b)**　　　**c)**

d)　　　**e)**　　　**f)**

Figure 1 - Schematic representation of different carbon allotropes: a) natural graphite; b) diamond; c) fullerene; d) single-walled carbon nanotube; e) multi-walled carbon nanotube; f) grapheneSource: Zarbin and Oliveira (2013).

Synthetic or processed carbonaceous materials are artificially obtained, that is, they present laboratory developed substances by the use of raw materials, such as: synthetic graphite, carbon fibers, glassy carbon, carbon fiber reinforced carbon composite (CRFC), composite carbon/carbon (C/C), cokes, coals, resins, piches and organic gases, being predominantly polygranular materials, composed of particles, fibers and binders of organic origin (MANTEL, 1968; MARSH, 1988; MARSH, HEINTZ and REINOSO, 1997; CGEE, 2010).

Graphite is one of the allotropic forms of naturally found carbon, being a classic example of a solid with lamellar structure, in which each carbon atom with sp2 hybridization is linked to three other atoms forming thousands of two-dimensional sheets (sheets) with the appearance of a hive (DRESSELHAUS, DRESSELHAUS and EKLUND, 1995). Each slide is called graphene, and stacking them, via van der Waals attractions, gives several planes of carbon atoms arranged in a hexagonal symmetry network (BELÉM, 2006; GEIM and NOVOSELOV, 2007; ZARBIN and OLIVEIRA , 2013). The graphite structure can be seen in Figure 2.

a)   **b)**
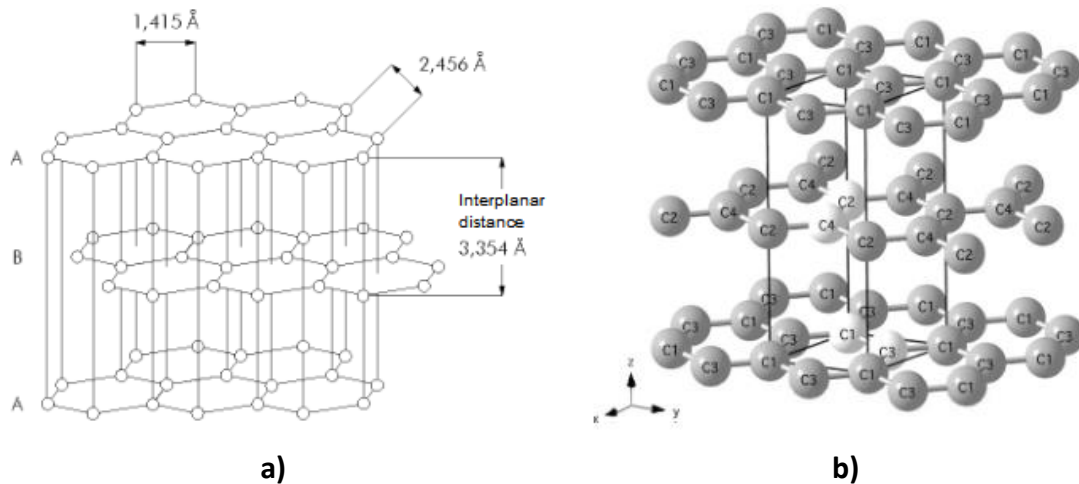
Figure 2 - Structural representation of graphite: a) crystalline arrangement; b) hexagonal structure
Source: OLIVEIRA *et al*., 2000; STANJEK and HÄUSLER, 2004.

More recently, with the consolidation and accelerated growth of nanoscience and nanotechnology, different physical, chemical and mechanical procedures have been developed for the preparation of nanometric materials. Among the methods, the mechanic, usually called high energy grinding, stands out for being easy to handle, efficient and quick to obtain nanometric powders. High energy ball milling is characterized by subjecting a material to repeated cycles of deformation, cold welding, grinding and fragmentation within a controlled atmosphere that causes high energy compressive impact forces (SURYANARAYANA, 1994; SURYANARAYANA, 2004). High energy mills produce shearing or impact on material particles by means of balls with powder at high speed generating a constant refinement of the material (MURTY and RANGANATHAN, 1998; CERQUEIRA, 2014). As a result, there is a reduction in particle size and structural variation of particles (SURYANARAYANA, 1994; SURYANARAYANA, 2004). This technique was developed around 1996 at the INCO Research Laboratory where Paul D. Merica, whose objective was to produce reinforced oxide dispersion in a nickel-based superalloy for gas turbine applications (MURTY and RANGANATHAN, 1998).

It should be noted, according to the literature, the scarcity of works related to obtaining graphite oxide using the high-energy ball mill (HEBM) of the SPEX type, in which few correspondents are found. To get an idea of the research using the SPEX vibratory mill in Brazil, a survey was carried out on the CAPES / MEC Portal page. As a result, there is only the research carried out by Junior in 2019, at the Federal University of Amazonas. Junior's research (2019) sought to synthesize commercial graphite using the high-energy SPEX mill to obtain graphene for application in supercapacitors. In this regard, the present research aims to obtain graphite oxide by means of MAE, even understanding that there is a finding that the procedure and theory issues have not yet been sufficiently explored in the specialized literature.

2. Materials and methods

2.1 Graphite Comminution

The proposed methodology for the execution of this work consisted of using the HEBM technique as a study route for obtaining graphite oxide. In this context, its reduction was studied through the following milling times: 30 minutes, 1 hour and 4 hours. The grinding process started with weighing the sample, and then the material (4g) was inserted into the cylindrical container (D = 2 ¼ ”and h = 3”) with a load capacity of up to 10g, along with two ½ inch steel balls to then start the mechanical comminution/amorphization process. Figure 3 illustrates the HEBM of the Prep 8000 M Mixer/Mill® line from Spex Sample.

Figure 3 - High power ball mill/homogenizer used in this work
Source: Suryanarayana (2001).

2.2 Scanning electron microscope (SEM)

For morphological investigation of the graphite samples, scanning electron microscopy (SEM) analysis was used. For this, a scanning microscope, brand TESCAN, model VEGA 3 SBH, was used under acceleration voltage of 15 kV. The analyzes were carried out at the Thematic Laboratory of Electronic Microscopy and Nanotechnology (LTMN) of the National Institute for Research in the Amazon (INPA).

2.3 X-ray diffraction (XRD)

The x-ray diffraction technique was used to characterize the crystalline structure of the precursor (material without grinding) and powders ground at different times (30 minutes, 1 hour and 4 hours). The samples were analyzed by a PANalytical diffractometer, model Empyrean, with Cu-Kα radiation (1.541838Å), operating at 40 kV voltage and 40mA current intensity. With a scanning range of 10° <2θ <80º of 2θ, and with a rate of 0.02º/min. The preparations and measurements of XRD samples were performed at the Materials Laboratory (LabMat) of the Federal University of Amazonas (UFAM). The average size and average width of the crystallites can be calculated using the formula developed by Scherrer (1918) (CULLITY and STOCK, 2001; XIAO et al., 2017).

$$L_a = \frac{k\lambda}{B\cos\theta} \tag{1}$$

$$L_c = \frac{k\lambda}{B\cos\theta} \tag{2}$$

Where Lc corresponds to the average size of the crystallite in the perpendicular direction to the basal planes of the graphite, K the form factor, 0.90 for the diffraction peaks (002) (STOBINSKI et al., 2014), La represents the average thickness of the crystallite 1.84 (Warren's constant) for bands (10) and (110) (WARREN, 1941), λ = radiation wavelength (Å), for copper radiation (Cu-Kα) of 1.541838Å,   = width at half the height of the most intensive diffraction peak (Figure 4) and θ is the peak Bragg angle (hkl), in degrees.
Interplanar distances (d002) can be calculated using the Bragg equation.

$$d_{002} = \frac{n\lambda}{2sen(\theta)_{002}} \tag{3}$$

The effective dimension of the crystallites (*L*) can be calculated from equation 4 (EMMERICH, 1995).

$$L = \left[\left(\frac{\pi}{4}\right).(L_a)^2.L_C \right]^{\frac{1}{3}} \tag{4}$$

Bowman (1956) explains that the widening of the crystalline planes is based on the combination of the widening of the plane due to the length of the crystallites , and due to the stresses arising from the fluctuation in the interplanar spacing value. The relationship between peak widening and deformation is defined as the structural stress (εc), along the c-axis and can be estimated by equation 5 (MIZUSHIMA, 1968).

$$\frac{1}{L_c} = L.\frac{\varepsilon_c}{2.d_{002}} \tag{5}$$

Depending on the Mering-Maire empirical formula, the graphite degree of graphite fibers can be calculated by equation 6 (XIAO et al., 2017).

$$G = \frac{0.344 - d_{002}}{0.344 - 0.3354} x100\% \tag{6}$$

The average number of layers per stack (N) can be calculated through the relationship between the size of the crystallite by the interplanar spacing between the graphite sheets (ALI UMAR et al., 2013). The average number of graphite sheets (N) can be represented by equation 7 (XIAO et al., 2019).

$$N = \frac{L_c}{d_{002}} \tag{7}$$

The packing density of the graphite layers can be expressed by Equation 8, as described by Popova (2017).

$$d = \frac{7,267}{d_{002}} \tag{8}$$

3. Results and discussion

3.1 Scanning electron microscope (SEM)

The graphite samples were characterized by scanning electron microscopy (SEM), where it was possible to monitor the morphological modification of commercial graphite as a result of mechanical grinding. Figure 4 shows the scanning electron microscopy images of the graphite before and after the mechanical comminution/amorphization process in the HEBM. The employment of SEM to analyze the structure of graphite is used to visualize the levels of comminution of the material on a 5μm scale.
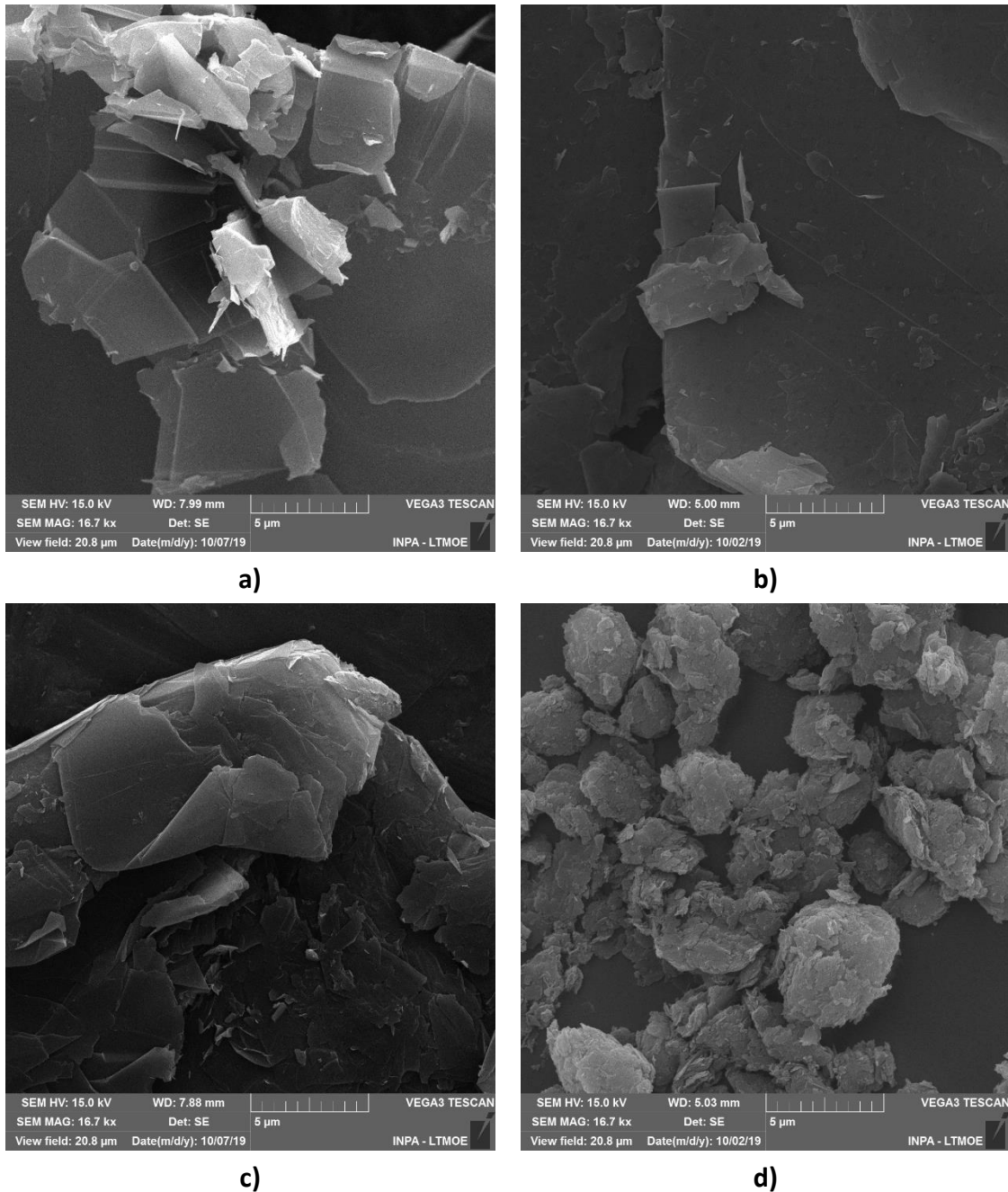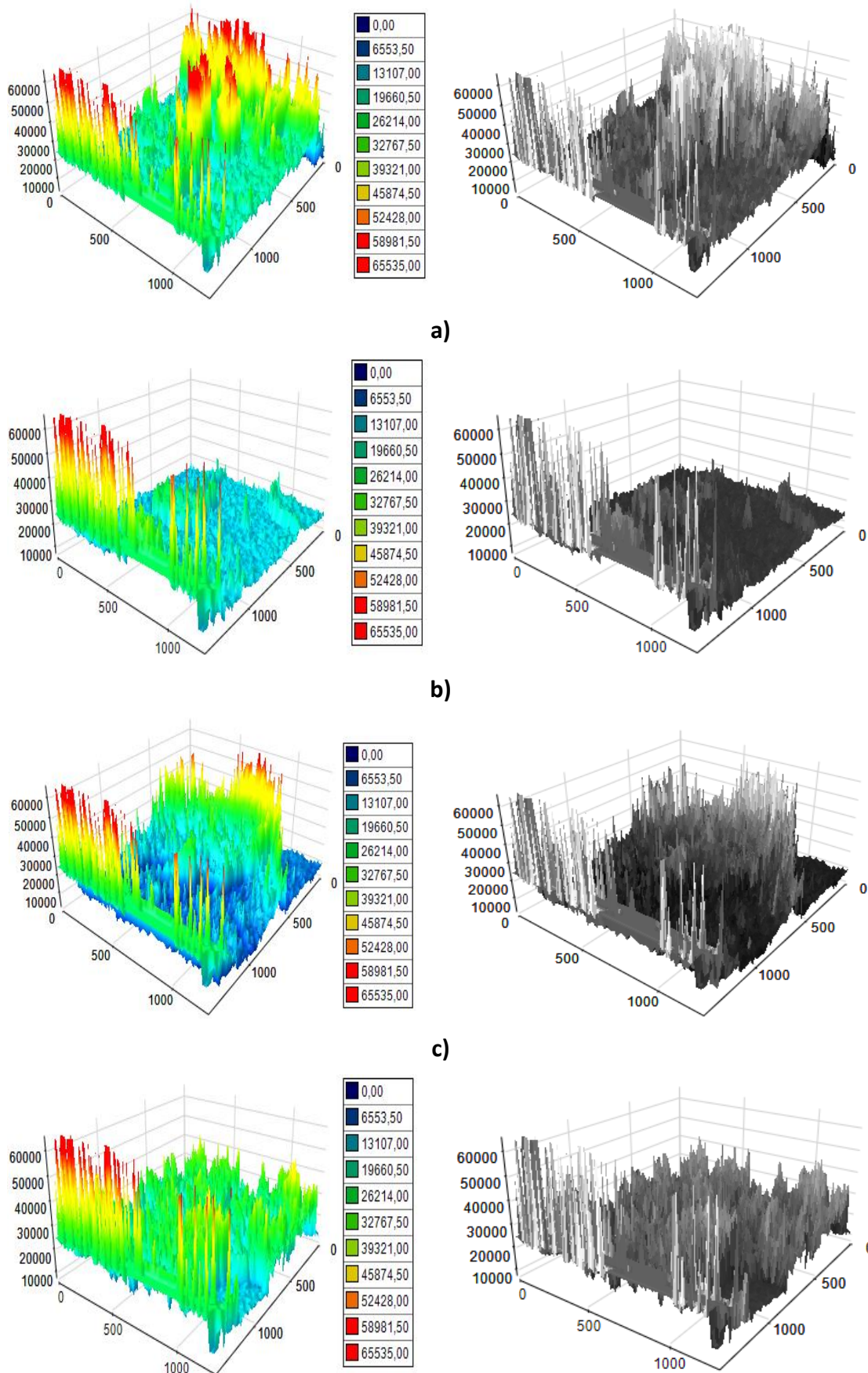
Figure 4 - Comparative micrographs of the precursor and ground powders: a) commercial graphite; b) graphite ground for 30 minutes; c) graphite ground for 1 hour; d) graphite ground for 4 hours.

Analyzing the images, Figure 4a shows the characteristic morphology of the graphite matrix, that is, it shows the structure of the graphite in well-defined plates in its crystalline state, with a smooth and uniform surface. Figure 4b shows the graphite comminuted for 30 minutes, where small changes in its crystalline structure can be seen. These changes are more significant in the graphite sample ground for 1 hour (Figure 4c). In Figure 4d there is a structure in the shape of spherical bodies (not perfectly spherical) after the mechanical grinding process for 4 hours. In particular, this almost spherical shape is characterized by the 4-hour mechanical amorphization process compared to commercial graphite, in which the graphite structure collapsed and deformed in a disorderly manner resulting in several pores of different sizes. It is also noted that the longer the grinding time, the greater the detachment between the plates. It is also worth mentioning the exfoliation of the material as the mechanical grinding time increases.

To better demonstrate the changes in the graphite samples due to the mechanical milling process, the Image-Pro Plus software was used to generate topographic images of the upper graphite surface, as shown in Figure 5.


a)

b)

c)

d)

Figure 5 - Peak intensity of surface micrographs: a) commercial graphite; b) graphite ground for 30 minutes; c) graphite ground for 1 hour; d) graphite ground for 4 hours.

Initially, in Figure 5a, the presence of intense peaks in the extremities is observed, which is characteristic of this material in its crystalline state. Figure 5b shows the evolution of the graphite sample in relation to the grinding time, in which the reduction of the peaks intensity in the central part to the extreme right of the surface is noticed. In Figure 5c, it is possible to verify the strengthening of the central and lateral peaks, indicating the structural change of the material. Observing Figure 5d of the graphite ground for 4 hours, the presence of peaks with medium intensity is observed in all the region of the microphotography. Also noteworthy is a more homogeneous distribution of the peaks in the matrix and differentiated color (closer to green) of the particles compared to the initial matrix and the matrices comminuted for shorter times, indicating that the degree of amorphization (non-crystalline layer) of the sample ground for 4 hours increased significantly due to the increase in the mechanical grinding time, which were initially totally crystalline. This suggests the formation of a new structure.

3.2 X-ray diffraction (XRD)

The analysis by XRD allowed to evaluate the structural difference between the precursor and the post-ground samples obtained by the mechanical amorphization process. Thus, for a better understanding of the obtained results, and at the same time to get a complete description of the behavior of the particles in relation to the mechanical effort, the diffractograms of the samples of commercial graphite and ground powders for the times of 15 minutes, 30 minutes, 1 hour and 4 hours were analyzed separately, as shown in Figure 6.
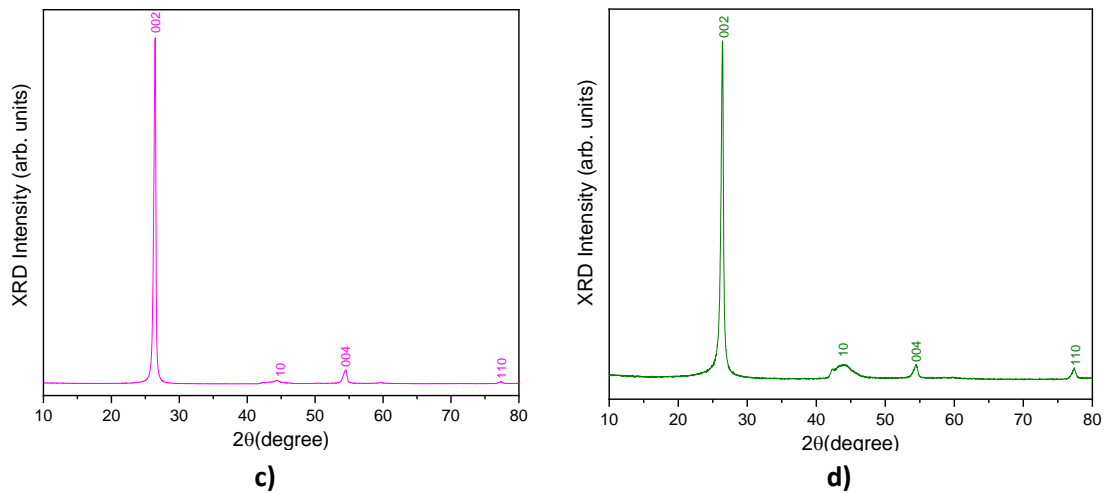

a)

b)
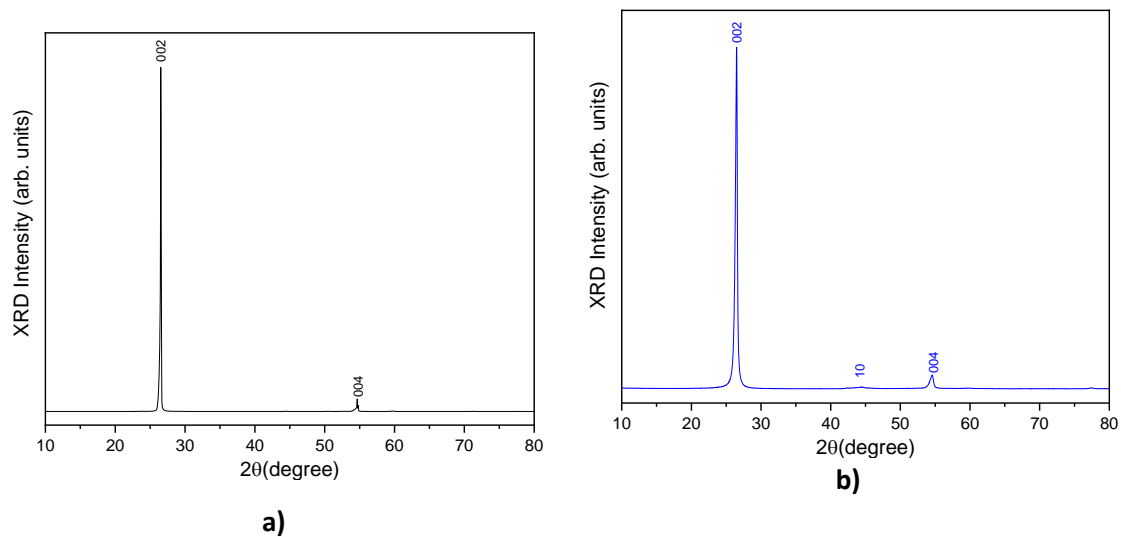
Figure 6 - X-ray diffractometers, individually analyzed a) commercial graphite, b) 30 min grinding, c) 1 hour grinding, e) 4 hours grinding.

In general, it appears that in all samples there is a crystalline plane (002), characteristic of graphite, located in the 26.6 ° region (IWASHITA et al., 2004; RODRÍGUEZ, 2015; LIU et al., 2017; GUO et al., 2017; VIEIRA et al., 2017) and (004) in 54.7º (RODRÍGUEZ, 2015), related to the average crystallite size (Lc) and pointing out to be a crystalline material. In Figure 6a, it is possible to check the planes (002), located at $2\theta = 26.6º$ and (004) at 54.7º, which are characteristic of the hexagonal carbon network, both being well defined and without apparent noise, in which it reflects greater organization of the graphite layers (RODRÍGUEZ, 2015; BANDI et al., 2019). Regarding Figure 6b, there is a reduction in the intensity of the crystalline plane (002) and a small displacement of the peak (004) by 54.6º, probably caused by the reduction of the refractive index and the decrease in the size of the crystallite. A timid principle of exfoliation of the material also stands out, where the peak (10) appears at 44.45º, indicating a structural change due to the mechanical grinding time (STOBINSKI et al., 2014) consolidating the appearance of two-dimensional structures, possibly with hybridization (sp2). The XRD spectrum of graphite ground for 1 hour (Figure 6c) shows a small decrease in intensity and widening of the peak (002), which is indicative of changes in ordering in relation to the original material. It was also possible to verify the consolidation of the peaks (004) and (10). Finally, the peak (110) appears, this diffraction peak indicates a higher process of exfoliation of the material and proof of graphite oxidation. In Figure 6d, there is a consolidation of the crystalline planes (10) and (110), and a differentiated widening of all the crystalline planes in relation to the other samples, pointing to a possible disorder in its structure, as well as the formation of a new crystalline structure and reduction of the average particle size. This behavior is the result of defects in the crystal and it can be caused by distortion of the graphite structure orientation. However, it is clear that the characteristic structure of the graphite was not destroyed, that is, there was no complete oxidation of it, a fact justified by the presence of the plane (002), showing an incomplete exfoliation of the graphite. Advancing the analysis of the results, the diffractograms were plotted together, as shown in Figure 7.
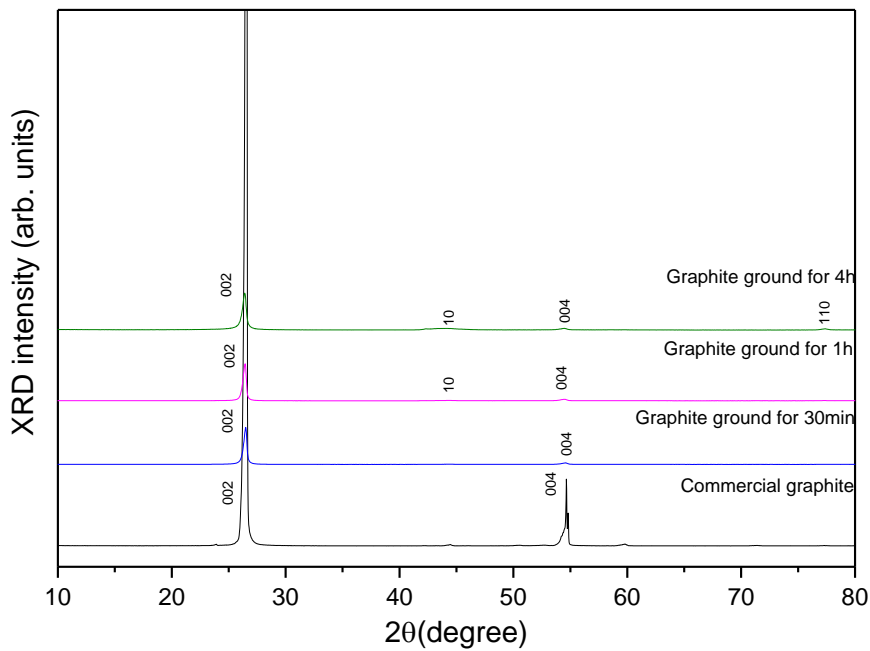
Figure 7 - X-ray diffractograms of commercial graphite and ground for different times: 15min, 30min, 1h and 4h

In Figure 7, a considerable reduction in the intensity of the crystalline plane (002) for the amorphized samples can be seen, when compared to commercial graphite, expressing a structure with a lower degree of organization and showing the graphite   exfoliation. It is also verified that no milling time studied was able to exfoliate and separate the graphite layers completely, however differences were detected in the intensity of the crystallinity peaks related to commercial graphite, as well as the appearance of the peaks (10) and (110) for graphite samples ground for 1 hour and 4 hours. The highest intensity of the characteristic peak (002) was obtained in the commercial graphite sample.

3.2.1 Characteristic of post-ground graphites

Table 1 presents the structural parameters of the precursor and for the respective materials ground for 30 minutes, 1 hour and 4 hours.

Table 1 - Structural parameters of graphite samples determined from the results obtained by means of diffractograms.

Sample	d_{002} [nm]	L_{c002} [nm]	L_{a10} [nm]	L_{a110} [nm]	L [nm]	ε_c	N	d [g/cm³]	G (%)
Graphite ground for 30 minutes	3,359	26,31	20,03	-	20,23	0,012747394	7,83	2,1635	94,34
Graphite ground for 1 hour	3,360	25,42	18,86	32,16	19,22	0,014017653	7,57	2,1627	92,81
Graphite ground for 4 hours	3,361	21,02	4,19	29,24	6,62	0,076303736	6,25	2,1621	91,77

In Table 1, it is possible to observe a progressive change in the graphite structure, as the grinding time increases, in which the mechanical comminution process disturbed the structural order of the precursor grafite. A fact observed by the gradual reduction of the average size of crystallites in the perpendicular direction to the basal planes, and the degree of graphitization and an increase in the specific surface area, as the grinding time increases.

Consolidating the values of reduction of the average size of the crystalline particles for better visualization of the results, we have the graph shown in Figure 8 that correlates the size of the crystallites (ordered) according to the grinding time (abscissa).
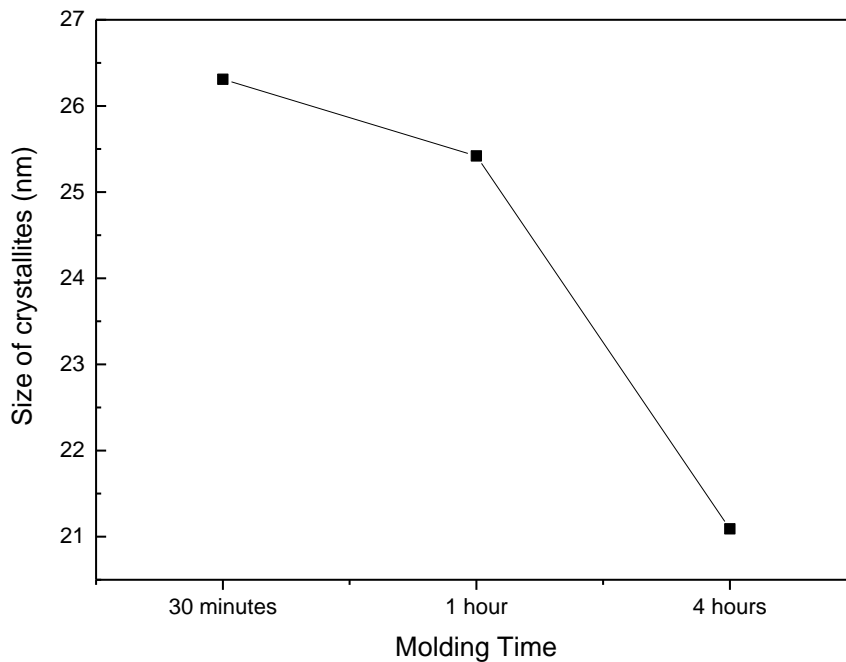

Figure 8 - Size of crystallites (L_{c002}).

According to the results of Figure 8, the graphite samples ground for 30 minutes, 1 hour and 4 hours show Lc002 of 26.31nm, 25.42nm and 21.02nm, respectively, that is, the higher the value, the more organized Lc002 the material is. In contrast, the longer the mechanical grinding time, the lower the value of Lc002 and G and, consequently, it translates into a less organized structure, an expected trend in the research in question, from the mechanical amorphization of graphite.

In Figure 9 the profile of the crystalline planes (002) of the graphite samples is compared. The respective values of Lc002 are also shown.
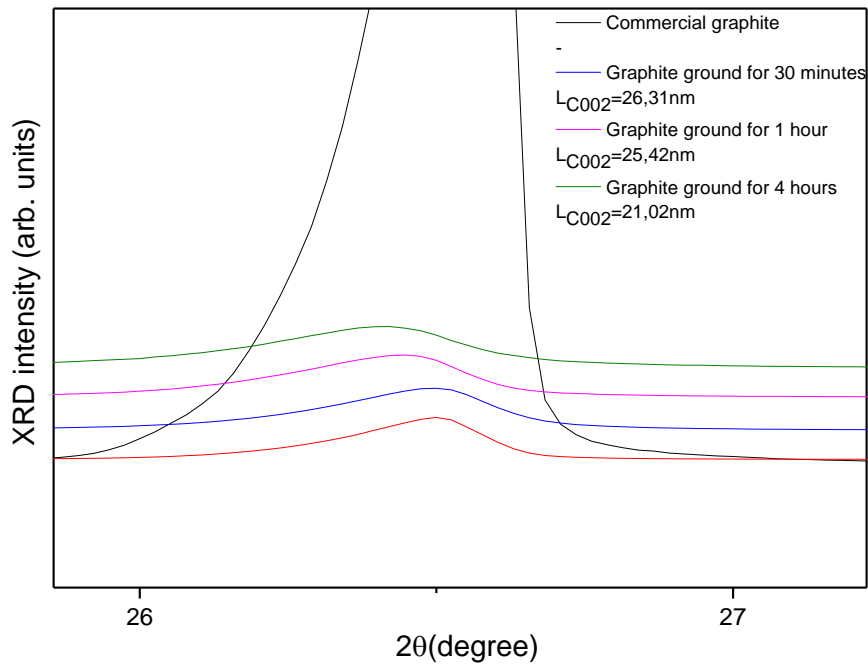
Figures 9 - Comparison of the intensity of the characteristic peaks (002) of the graphite samples.

When analyzing the profiles of the graphite peak (002) in Figure 9, it can be seen that the samples have different dimensions for the graphite band (002), mainly in intensity and displacement, exposing different degrees of graphitization. It is also possible to observe the micronization trend after the gradual grinding process in relation to the precursor. The high-energy mechanical grinding process, in addition to favoring changes in the properties of materials, is also responsible for a progressive process of mechanical amorphization of graphite particles. Thus, increasing the grinding time can promote comminution/amorphization of the particles, reducing their average size and increasing the specific surface area of the material. In this way, longer mechanical grinding times play a fundamental role in increasing the non-crystalline fraction, since the shearing action and the impact of the spheres on the crystalline particles, from the surfaces, cause a reduction in the average size of the crystalline particles (CARREÑO, 2008).

Also noteworthy are the results of the sample ground for 4 hours, in which it is possible to observe the smallest crystallite size recorded, indicating the structural change of the material as well.

Advancing in the results analysis, Figure 10 shows the results of the distances between the planes (d002) of the graphite samples as a function of the grinding time.
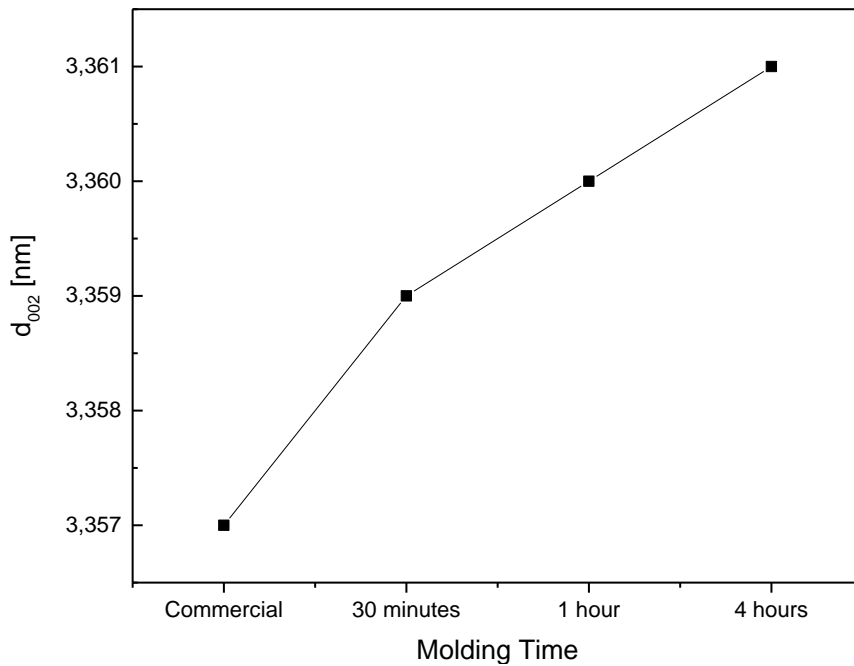
Figure 10 - Interplanar distance of samples as a function of grinding time.

Analyzing the graph in Figure 10, it is observed that the samples of commercial graphite, graphite ground for 30 minutes, 1 hour and 4 hours show d002 of 3.359nm, 3.360nm and 3.36108nm, respectively. That is, the post-ground samples have diffraction planes displaced to smaller angles, as the grinding time increases. According to Rodríguez (2015), the graphite d002 interplanar spacing is referred to by the value of 3.35nm, explaining a high crystallinity characteristic of the material. Therefore, the structural change of graphite through the grinding process is noticeable. Thus, increasing the grinding time, in general, causes the expansion of the blades present in the graphite structure. These changes in characteristic peaks (002) are more clearly shown   in Figure 11.
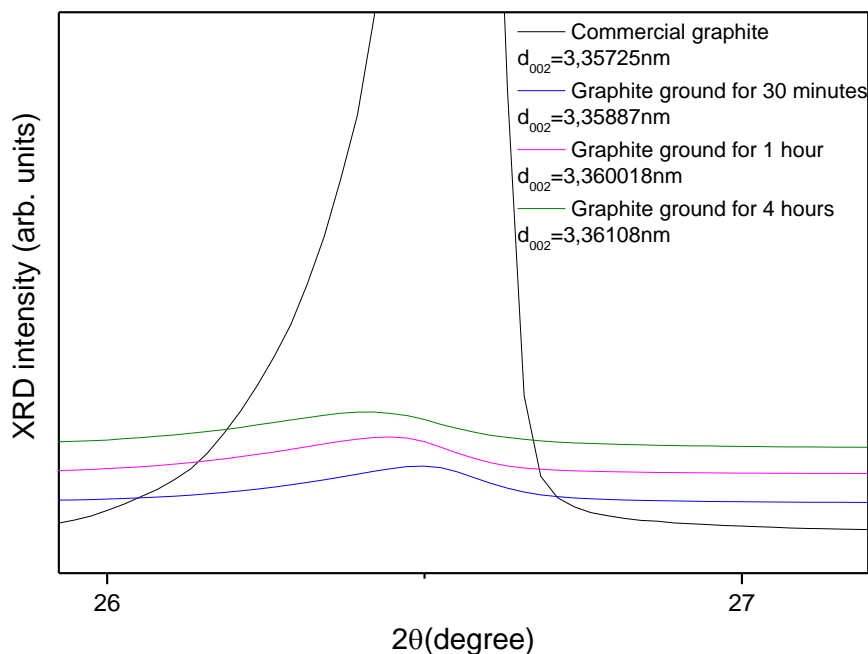

Figure 11 - Comparison of the d_{002} interplar distance of the graphite samples.

In Figure 11, an increase in the interplanar distance of post-ground samples compared to the precursor can be seen . However, this increase was slight in relation to the precursor, which indicates that there was no process of complete exfoliation of its structure to obtain graphite oxide.

4. Conclusion

This work aimed to study the obtaining of graphite oxide through the simple mechanical grinding process, without using oxidizing agents or concentrated acids. According to the XRD and SEM tests, the grinding process disturbed the structural order of the precursor graphite, in which both results agree that the structural change of the graphite is proportional to the increase in grinding. In this way, there is an interrelation between the results of XRD and the results of micrographs of the surface and SEM, in which there is a structural change in the graphite, as the mechanical grinding time increases. Although the structural changes are noticeable, as the mechanical grinding time increases, no time studied was able to exfoliate and separate the graphite layers completely.

5. Acknowledgement

6. References

MANTEL, C. L. Carbon and Graphi-te Handbook. Interscience, v. 1, 1968.

MARSH, H. Introduction to Carbon Science. Butterworth & Co, v. 1, 1989.

SAVAGE, G. Carbon-carbon composites. Chapman & Hall (1993).

CGEE - Centro de Gestão e Estudos Estratégicos. Materiais avançados no Brasil 2010-2022. Centro de Gestão e Estudos Estratégicos, 2010.

ZARBIN, A. J. G.; OLIVEIRA, M. M. Nanoestruturas de carbono (nanotubos, grafeno): quo vadis? Química Nova, v. 36, n. 10, p. 1533-1539, 2013.

MARSH, H.; HEINTZ, E.; REINOSO, F. R. Introduction to Carbon Technologies. University of Alicante, Alicante/Spain, v. 1, 1997.

DRESSELHAUS, M. S.; DRESSELHAUS, G.; EKLUND, P. C. Science of Fullerenes and Carbon Nanotubes. Academic Press: San Diego, 1995.

BELÉM, J. Caracterização Mineralógica, Física e Termobarométrica de Minérios de Grafita da Província Grafítica Bahia-Minas. Dissertação - Universidade Federal de Minas Gerais. UFMG. Programa de Pós-Graduação do Instituto de Geociências. Belo Horizonte, 2006.

GEIM, A.K.; NOVOSELOV, K.S. The rise of graphene. Nature Materials. v. 6, p. 183-191, 2007.

OLIVEIRA, I. R.; STUDART, A. R.; SILVA JÚNIOR, F.; PANDOLFELLI, V. C. Artigo revisão: Estabilização de suspensões aquosas contendo grafite. Cerâmica, v. 46, n.300, p. 186-195, 2000.

STANJEK, H.; HÄUSLER, W. Basics of X-ray diffraction. Hyperfine Interactions. v. 154, p. 107-119, 2004.

SURYANARAYANA, C. Structure and properties of nanocrystalline materials. Bulletin of Materials Science, v. 17, n. 4, p. 307–346, 1994.

SURYANARAYANA, C. Mechanical Alloying and Milling Mechanical Engineering. Progress in Materials Science, v. 46, n. 1–2, p. 488, 2004.

MURTY, B. S.; RANGANATHAN, S. Novel materials synthesis by mechanical alloying/milling. Journal International Materials Reviews. v. 43, n. 3, p 101-141, 1998.

CERQUEIRA, V. R. Síntese e Sinterização de pós-compósitos de alumina-boretos de alta dureza por moagem de alta energia. Tese de Doutorado - Programa de Pós-graduação em Ciência e Engenharia de Materiais, Universidade Federal de São Carlos, São Paulo, 2014.

Junior, A. J. C. P. Síntese de grafeno por moagem de alta energia para aplicação em supercapacitores. Dissertação (Mestrado em Ciência e Engenharia de Materiais) - Universidade Federal do Amazonas, Manaus, 2019.

CULLITY, B. D.; STOCK, S. R. Elements of X-ray Diffraction, 3ª ed, Prentice Hall: Upper Saddle River, 2001.

XIAO, M.; LI, N.; MA, Z.; SONG, H.; LU, K.; LI, A.; MENG, Y.; WANG, D.; YAN, X. The effect of doping graphene oxide on the structure and property of polyimide-based graphite fibre. RSC Advances. v. 7, n. 89, p. 56602–56610, 2017.

STOBINSKI, L. LESIAK, B.; MALOLEPSZY, A.; MAZURKIEWICZ, M.; B. MIERZWA, B.; ZEMEK, J.; P. JIRICEK, P.; BIELOSHAPKA, I. Graphene oxide and reduced graphene oxide studied by the XRD,TEM and electron spectroscopy methods. Journal of Electron Spectroscopy and Related Phenomena, v. 195, p. 145–154, 2014.

WARREN, B. E. X-Ray Diffraction in Random Layer Lattices. Physical Review, v. 59, n. 9, p. 693–698, 1941.

EMMERICH, F. G. Evolution with heat treatment of crystallinity in carbons. Carbon, v.33, n. 12, p. 1709-1715, 1995.

BOWMAN, J. C. Proceedings of the 1st and 2ndConference on Carbon. In: CONFERENCE ON CARBON. New York: Buffalo University, 1956.

MIZUSHIMA, S. On true crystallite thickness and interlayer spacing in graphitic carbons. Tanso, v. 1968, n, 52, p. 9-12, 1968.

ALI UMAR, M. I., YAP, C. C., AWANG, R., HJ JUMALI, M. H., MAT SALLEH, M., & YAHAYA, M. Characterization of multilayer graphene prepared from short-time processed graphite oxide flake. Journal of Materials Science: Materials in Electronics, v. 24, n. 4, 1282–1286, 2013.

XIAO, M; ZHANG, X.; XIAO, W.; DU, J.; SONG H.; MA, Z.; The influence of chemical constitution on the structure and properties of polyimide fibre and their graphite fibre. Polymer. v. 165, p. 142–151, 2019.

POPOVA, A. N. Crystallographic Analysis of Graphite by X-Ray Diffraction. Coke and Chemistry. v. 60, n. 9, pp. 361–365, 2017.

IWASHITA, N.; PARK, C.R.; FUJIMOTO, H.; SHIRAISHI, M.; INAGAKI, M. Specification for a standard procedure of X- ray diffraction measurements on carbon materials. Carbon, v. 42, p. 701-714,

2004.

RODRÍGUEZ, B. A. G. Síntese e caracterização de grafeno oxidado e nanofitas de carbono e estudos de suas possíveis aplicações. Tese de Doutorado - Programa de Pós-Graduação em Ciência de Materiais, Universidade Federal de Pernambuco, Recife, 2015.

LIU, Y., JIN, W., ZHAO, Y., ZHANG, G. Enhanced Catalytic Degradation of Methylene Blue by ε-Fe2O3/graphene Oxide via Heterogeneous Photo-Fenton Reactions. Applied Catalysis B: Environmental, v. 206, pp.642–52, 2017.

GUO, S., YUAN, N., ZHANG, G., YU, J. C. Graphene Modified Iron Sludge Derived from Homogeneous Fenton Process as an Efficient Heterogeneous Fenton Catalyst for Degradation of Organic Pollutants. Microporous and Mesoporous Materials, v. 238, pp.62–68, 2017.

VIEIRA, M. A.; FRASSON, C. M. R.; COSTA, T. L. G.; CIPRIANO, D. F.; SCHETTINO JR., M. A.; CUNHA, A. G.; FREITAS, J. C. C. Estudo através de rmn de 13c no estado sólido sobre a síntese de oxido de grafite utilizando diferentes precursores grafíticos. Química Nova, v.40, n.10, p.1164-1171, 2017.

BANDI, S; RAVURI, S; PESHWE, D.R; SRIVASTAV, A.K. Graphene from discharged dry cell battery electrodes, journal of hazardous materials. Journal of Hazardous Materials. v. 366, p. 358-369, 2019.

STOBINSKI, L. LESIAK, B.; MALOLEPSZY, A.; MAZURKIEWICZ, M.; B. MIERZWA, B.; ZEMEK, J.; P. JIRICEK, P.; BIELOSHAPKA, I. Graphene oxide and reduced graphene oxide studied by the XRD,TEM and electron spectroscopy methods. Journal of Electron Spectroscopy and Related Phenomena, v. 195, p. 145–154, 2014.

CARRENO, N. L. V.; GARCIA, I. T. S.; LEITE, E. R.; SANTOS, L. P. S.; KEYSON, D.; LONGO, E.; FAJARDO, H. V.; PROBST, L. F. D.; FABBRO, M. T. Nanocompósitos cerâmicos a partir do processo de moagem mecânica de alta energia. Química Nova, v. 31, p. 962-968, 2008.